Design and Performance of an Annular Magnetoplasmadynamic Thruster

D. J. Heimerdinger*
Institute for Defense Analyses, Alexandria, Virginia 22311
and
M. Martinez-Sanchez†
Massachusetts Institute of Technology, Cambridge, Massachusetts 02139

In this paper both theoretical and experimental results are presented that demonstrate the effects of electrode geometry on the operation of the magnetoplasmadynamic (MPD) arcjet and describe the "onset" phenomenon not as a single phenomenon but as two distinct phenomena—one in which thruster efficiency is drastically reduced due to an anode depletion mechanism and the other when thruster lifetime is decreased due to enhanced erosion. Theory and data both show that the electrode current concentrations can be locally changed by varying the channel's interelectrode separation. The experiment (conducted on a large radius annular geometry) shows a clear separation between an anode depletion description of onset (caused by the radial component of the thrust vector), indicated by the growth of a large anode voltage drop, and onset indicated by the appearance of unsteady large amplitude voltage oscillations which are attributed to convective motion of large concentrated anode arcs.

Nomenclature

A	=	cross-sectional area
B	=	magnetic induction
b	=	thrust parameter
e	=	fundamental charge
G	=	geometry correction factor
H	=	interelectrode separation
J	=	total current
j	=	current density
L	=	thruster length
m_i	=	ion mass
$\dot{m}$	=	mass flow rate
R	=	gas constant
r_a	=	anode radius
r_{co}	=	radius of the cathode at the channel entrance
T	=	mean temperature
t	=	time
u	=	mean mass velocity
u_e	=	exhaust velocity
V_{emf}	=	voltage due to the back emf
V_T	=	terminal voltage
x	=	axial coordinate
y	=	transverse coordinate
β	=	Hall parameter
ΔV_{anode}	=	anode voltage drop
η	=	efficiency
μ_o	=	permeability of free space
Π	=	total pressure
ρ	=	plasma density
σ	=	plasma electrical conductivity
*	=	onset condition

Introduction

COAXIAL self-field MPD thrusters need to operate at very high mean power densities for the useful back electromotive force (emf) to exceed the Ohmic voltage drop in the plasma and the near-electrode drops. This high power density guarantees sufficient ionization to put the plasma in the Coulomb-dominated regime. Beyond this point, additional ionization may detract from the overall efficiency since bulk recombination in the nozzle is unlikely. It is, therefore, important to reduce the local Ohmic dissipation (which feeds the ionization process) to as low a value as possible within the constraints of providing sufficient magnetic interaction and ionization.

For this reason, it would be desirable to have the ability to specify or control the distribution of current throughout the MPD channel. A uniform current distribution, hypothesized as providing approximately (at least locally) the maximum ratio of mechanical work to total input energy,[1] might help increase thruster efficiency by reducing frozen losses.

An additional potential benefit of a uniform current distribution is a reduction of localized electrode damage where current normally concentrates, typically at the cathode base and at the anode lip. However, more needs to be done to verify this point, since, for instance, anode voltage drops in an arcing mode are known to fall as the current density increases.[2]

Operation at these high power densities has also been characterized by a phenomenon known as "onset." At onset, MPD arcjet performance has been seen to degrade rapidly. This limit, characterized by a large increase in terminal voltage accompanied by large amplitude voltage oscillations, has been linked to thruster erosion, decreased thruster efficiency, and unsteady operation.[3–5] This limit has prevented MPD arcjets from operating at high thrust levels and efficiencies.

Several mechanisms for onset have been postulated. These include anode starvation,[6] plasma instabilities,[7] cathode arcing,[8] and full ionization.[9] However, they fail to fully describe the observable phenomenology associated with the onset limitation.

These considerations prompted us to develop an approximate design theory[10,11] in which current distribution is an input and channel interelectrode separation then results. Additional theory was also developed to help understand the phenomenology of onset and provide a guide for its prediction. An experiment was also conducted to complement the theoretical work at MIT. This paper presents an outline of the theory and the experimental results along with a discussion of their implications.

Presented as Paper 88-039 at the 20th DGLR/AIAA/JSASS International Electric Propulsion Conference, Garmisch-Partenkirchen, Germany, Oct. 3–6, 1988; received March 15, 1990; revision received Dec. 10, 1990; accepted for publication Dec. 13, 1990.

*Professional Staff, Systems Evaluation Division. Member AIAA.
†Associate Professor, Department of Aeronautics and Astronautics. Member AIAA.

MPD Arcjet Design

The reader is referred to Refs. 10 and 11 for a detailed description of the design theory. In brief, the theory details the role of geometry on the distribution of current throughout the MPD channel, and at the same time, provides information on the two-dimensional structure of the plasma throughout the discharge channel.

The effect of geometry on the internal distribution of current can be illustrated from a simplified version of Ohm's law written in a single dimension

$$j = \frac{\sigma}{1 + \beta^2}(E - uB) \tag{1}$$

In the absence of significant electrode falls, the local electric field, E, is approximately the ratio of the terminal voltage to the interelectrode separation, V/H. At the entrance of the MPD arcjet, the back emf is small due to the low velocity of the plasma. At the exit plane of the channel, the back emf may not be low due to current convection, but at the electrode surface, current termination is an eventuality and this transition to zero magnetic field provides a region where the local electric field is supported resistively, often resulting in very high current concentrations. In order to prevent these large current concentrations in these regions, the local electric field must be decreased. This may be accomplished by increasing the interelectrode separation.

Baksht[6] and Hugel,[4] both showed that the MPD discharge has a two-dimensional structure which cannot be neglected in evaluating the ultimate performance of the discharge. As a result, this model incorporates the appropriate terms detailing the effects of a nonconstant Hall parameter.

The model is based on a magnetohydrodynamic formulation where the basic limitations are: a) steady-state, b) two-dimensional geometry, c) constant conductivity (constant temperature), d) constant anode and cathode drops (hence equipotential walls), e) neglect of the initial ionization region (which for high values of $J^2/\dot{m}$ is assumed to be small), and f) relatively small transverse property gradients (slender channel geometry). From these assumptions, the MHD equations of motion can be simplified to the following induction equation

$$\mu_o \sigma \rho u \frac{\partial}{\partial x}\left(\frac{B}{\rho}\right) = \frac{\partial^2 B}{\partial y^2} + \frac{\mu_o m_i \sigma}{e\rho^2}\frac{d\Pi}{dx}\frac{\partial \rho}{\partial y} \tag{2}$$

where Π is the sum of the thermodynamic and magnetic pressures and is independent of the transverse coordinate

$$\Pi(x) = \rho RT + \frac{B^2}{2\mu_o} \tag{3}$$

The term on the left hand side of Eq. (2) is the convection of the magnetic field and density; the first term on the right is the transverse diffusion of magnetic field; and the second term arises from the nonzero Hall parameter.

Equation (2) is solved in an approximate manner. The approach used started from a zeroth-order solution in which an assumed axial electric field cancels the axial current, thus guaranteeing zero transverse variations. This results in the quantity B/ρ becoming a convective constant, which enables direct algebraic solution for the various zero'th-order flow variables. This solution was then modified by a perturbation scheme which determined the transverse variations created by relaxing the axial field to zero. Within the limitations of the theory, we were then able not only to calculate the flow area variation required for a specified axial distribution of current density, but also to predict the conditions at which transverse density gradients grow to the point of depleting the anode wall.

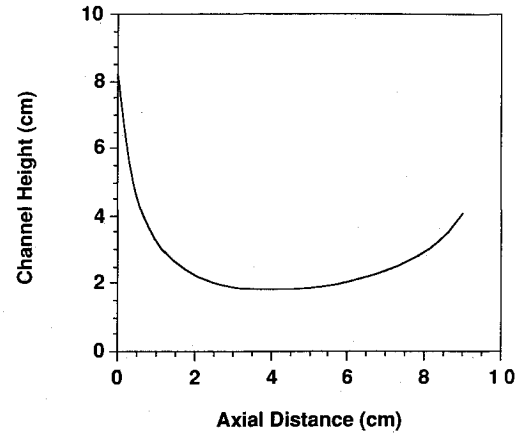

Fig. 1 Calculated electrode separation.

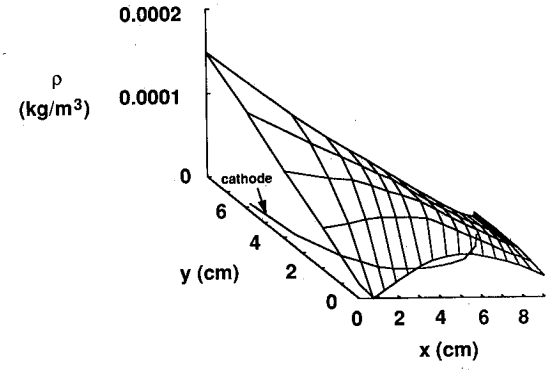

Fig. 2 Calculated density distribution in the theoretical MPD arcjet channel.

For the experimental channel, the chosen design conditions were:

Mass flow rate	$= \dot{m} = 4$ g/s (Argon)
Current	$= J = 42$ kA
Length	$= L = 9$ cm
Throat height	$= H = 1.9$ cm
Current distribution	= Uniform to zeroth order

Figure 1 shows the theoretically determined channel shape, which can be seen to be convergent-divergent. The presence of axial current, which somewhat distorts the imposed uniform zeroth-order current distribution, is responsible for the depletion of charge carriers in the anode region shown in Fig. 2. Anode depletion is readily observed in this channel based on the specified design conditions, but it only occurs in a small portion of the channel just upstream of the channel throat.

Experimental Apparatus

The theory is two-dimensional, but in order to avoid sidewall problems (and to keep with standard design practice), we decided to use a cylindrical geometry, with only minor adjustments to the theory. To reduce the inaccuracy introduced by the cylindrical effects, the mean radius of the device was chosen rather large (6.3 cm). In this geometry, the anode was made purely cylindrical for convenience, with the cathode taking up the required contour. The calculated anode depletion current was only slightly above the design value of 42 kA. For comparison, a form of Baksht's theory[6] modified for cylindrical effects, predicts anode depletion at 41 kA.[11]

To verify the effects of geometry on the discharge, two other channels were built. One had constant interelectrode separation (constant area channel—CAC), at the same value as the throat of the fully-flared channel (FFC), and the par-

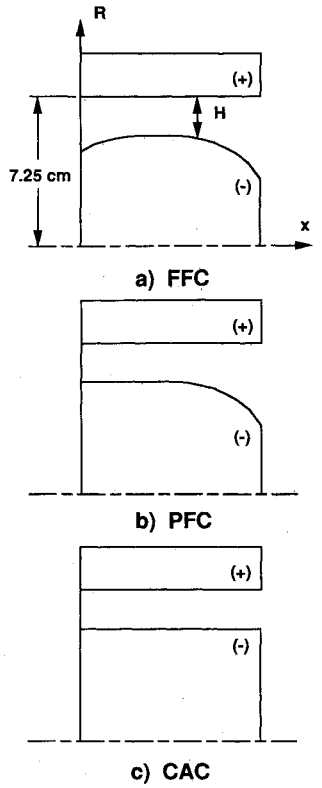

x	Channel Height		
	CAC	PFC	FFC
0.00	1.90	1.90	2.66
0.60			2.36
1.20			2.20
1.80			2.01
2.40			1.93
3.00			1.91
3.60			1.90
4.20			1.90
4.80			1.90
5.40		1.94	1.94
6.00		2.05	2.05
6.60		2.22	2.22
7.20		2.45	2.45
7.80		2.79	2.79
8.40		3.28	3.28
9.00	1.90	4.03	4.03

Note: All measurements are in centimeters.

Fig. 3 Three experimental MPD arcjet geometries.

tially flared channel (PFC) which had the theoretical contour downstream of the throat and a constant upstream cross-section. In addition, the FFC was built with less drastic upstream area variation than required by theory, because theory itself also indicated that dissipation near the entrance would be too low to support rapid ionization of the entering flow. The three channel geometries are diagrammed in Fig. 3.

In order to provide for quasi-steady operation, the MPD arcjet was powered by an eight stage inductor-capacitor (L-C) ladder capable of storing 400 kJ. It had been configured to provide a current pulse of over 60 kA for a duration lasting approximately 300 μs.

The arcjet was situated in a stainless-steel vacuum tank 7 m long and 0.6 m in diameter. Six fast acting valves provided a gas pulse from a reservoir directly behind the arcjet channel. Upon command, these valves fired simultaneously. After an appropriate delay to ensure steady-state flow, the discharge was initiated into an ambient pressure less than 10^{-4} torr, and the data acquisition system is triggered.

Thruster diagnosis was accomplished primarily by the use of probes. Current was measured by time integrating the measured transient magnetic field and voltage was measured either by a high impedance differential voltage probe or a floating potential probe. A large Rogowski loop was used to measure the total thruster current and a Tektronix 1000:1 voltage probe was used to measure the terminal voltage. Internal distributions of magnetic field and floating potential were also obtained by probing. The magnetic field was measured from a small 1/16 in. Rogowski loop placed in a quartz tube located directly in the plasma flow. The floating potential was measured by a single Langmuir probe also placed in the plasma stream.

In addition to this probing, spectroscopic emission measurements at the exit plane of the thrusters were made. A 1.26 m Czerny-Turner spectrometer with a Silicon Intensified Target (SIT) digitizing camera at its exit slit were used for this purpose. For a more detailed description of the optical analysis, refer to Kilfoyle.[12]

Terminal Characteristics and Operating Regimes

Initial tests with the CAC at the nominal 42 kA, 4 g/s of argon operating point showed erratic and often asymmetric ignition. This was attributed to insufficient inlet ionization, coupled with the large nonsegmented electrode perimeter. Conditioning by repeated discharges did improve the ignition characteristics, but it was also found that increasing the current up to about 60 kA still did not produce the anticipated unsteadiness typical of "onset." As a consequence, most of the detailed data were taken at this higher current level.

Figure 4 shows that the terminal voltages were similar in all three channels, although measurably lower in the constant area case. Error bars reflect the total uncertainty of the voltage measurement due to probe noise and voltage oscillations. More detailed examination revealed that, starting at about 30–40 kA, the anode voltage drop became a substantial part of the total voltage. This is shown in Fig. 5 for the FFC. A sharply increased anode voltage drop has been linked in the past to anode depletion,[4,5] i.e., a plasma density near the anode which is insufficient to diffusively supply the local current density. Thus, even though no large-scale unsteadiness was detectable below 60 kA, it is quite probable that the anode was depleted at 30–40 kA not far from the theoretical predictions, particularly those of the modified Baksht theory.

Although anode depletion (also known as "anode starvation") is suggested, the mode of near-anode conduction between, say 35 and 60 kA is still not clear from these data. More detailed measurements of the near-anode region, detailing the local plasma density, temperature, and electric field are necessary before any detailed hypotheses are forwarded.

The growth of a potential drop near the anode acts to decrease MPD thruster performance by limiting the thruster efficiency. If the voltage associated with the back emf is considered to be a measure of the exhaust kinetic energy, then the thruster efficiency can be written as

$$\eta = \frac{V_{\text{emf}}}{V_T} = \frac{V_T - \Delta V_{\text{anode}} - \Sigma \Delta V_i}{V_T} \tag{4}$$

where ΔV_i is the other contributors such as the Ohmic contribution and the cathode voltage fall.

In the FFC, the ratio $\Delta V_{\text{anode}}/V_T$ is approximately 0.5 at 30 kA and rises to over 0.9 between 40 and 50 kA. This shows that the anode voltage drop dominates the discharge voltage and drastically reduces the thruster's efficiency.

As the current was increased past about 60 kA, there was a distinct transition to an anode arcing mode of operation. This operation is characterized by fairly regular (50 kHz) fluctuations in the terminal voltage as illustrated in Fig. 6. Intense luminous anode spots are also seen in photographs taken during the discharge and by their erosion tracks, which are apparent only after this transition and span the length of

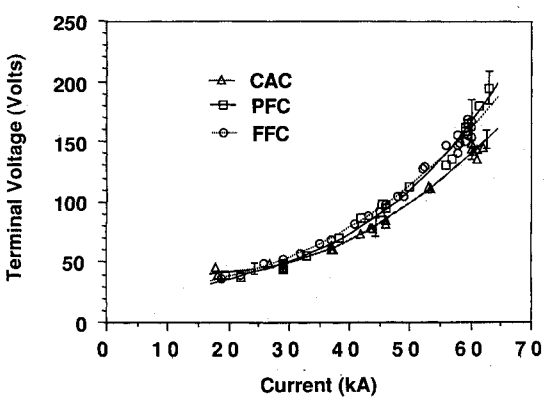

Fig. 4 Experimental voltage-current characteristics for the three channels.

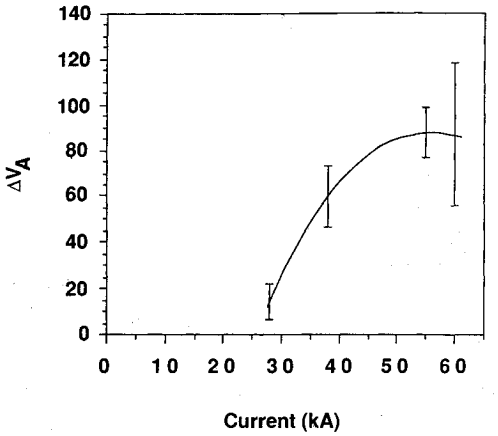

Fig. 5 Experimentally determined anode-region voltage drop (Anode to 3 mm from the Anode) at x = 4.3 cm in the FFC.

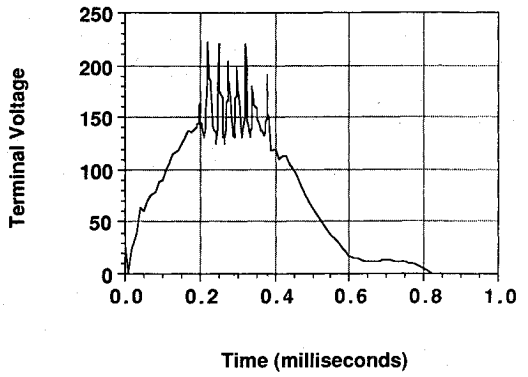

Fig. 6 Terminal voltage fluctuations in the FFC at 60 kA.

the channel.[10] This oscillatory behavior was most distinct in the FFC, but was also exhibited at a higher current in the PFC as seen in Fig. 7. At no time was this oscillatory voltage noted for the CAC which was tested up to 64 kA. In fact, for the CAC, there was only a hint of unsteadiness at the highest recorded current (64 kA) while the FFC showed a sharp transition to unsteady conditions around 60 kA. There were also indications of a high degree of single ionization at the high current levels but no discernible second ionization in the thruster's exhaust.[12,13]

Turchi has postulated that as full ionization is approached the arc will be forced to erode material from confining surfaces in some unspecified manner in order to strike a power balance, and that this gives rise to the onset syndrome.[8] An alternative possibility near full ionization is the occurrence of a fast-growing electrothermal instability[14,15]; once the ionization energy sink is largely removed, concentration of current in some area will lead to an electron temperature excursion there, creating a locally greater conductivity and thus reinforcing itself. These hypotheses lead to the possible conclusion that the lack of oscillations in the CAC may be the result of stronger diffusion of charged pairs (ambipolar diffusion), due to the smaller transverse dimension, which provides for an ionization energy sink. Another possibility is that the adverse pressure gradient imposed by the transverse component of the $\vec{j} \times \vec{B}$ force inhibits the flow less in the flared channels than in the CAC. The cathode flare allows for greater expansion and, therefore, lowered anode densities which may not be sufficient to support a diffuse discharge.

Both of these hypotheses are not verifiable but are consistent with the data. Although enhanced conductivity associated with thermal runaway and a large adverse pressure gradient would tend to favor a higher operating voltage for the CAC over the PFC and the FFC, the higher expected

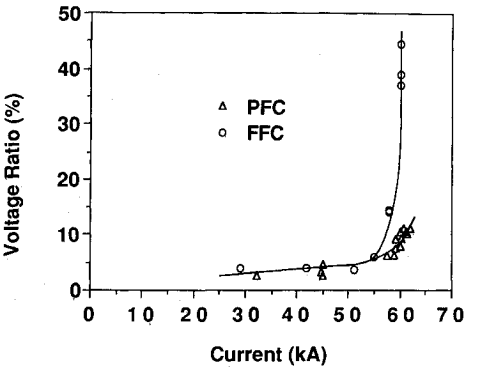

Fig. 7 Ratio of the peak-to-peak oscillatory voltage to the terminal voltage as a function of thruster current in the FFC and the PFC.

back emf in the flared channels opposes this trend. The back emf can be approximated by calculating the exhaust velocity in each of the thrusters. In Heimerdinger,[11] approximate equations for the thrust for the three channels are derived. From these equations the exhaust velocity can be calculated. The thrust equations all have the form

$$T = \frac{\mu_o}{4\pi} J^2 \left(\ln \frac{r_a}{r_{co}} + G \right) \tag{5}$$

where G is a correction term associated with electrode flaring. The exhaust velocity (or specific impulse) follows as

$$u_e = \frac{I_{sp}}{g} = \frac{\mu_o}{4\pi} \left(\ln \frac{r_a}{r_{co}} + G \right) \frac{J^2}{\dot{m}} \tag{6}$$

For the three channels, this leaves

$$\text{CAC: } T = 3.03 \times 10^{-8} J^2 \tag{7}$$

$$\text{PFC: } T = 3.75 \times 10^{-8} J^2 \tag{8}$$

$$\text{FFC: } T = 3.53 \times 10^{-8} J^2 \tag{9}$$

where the thrust is in Newtons and the current is in kiloamps. As expected, both the PFC and the FFC have higher exhaust velocities and specific impulses than the CAC at a given current level, so that the back emf of the two flared channels is higher. The PFC has a higher thrust, exhaust velocity, and specific impulse than the FFC due to a substantial negative contribution in the converging channel section. This result contradicts that by Martinez-Sanchez[16] in that a convergent inlet increases performance more than a divergent downstream section. The reasons for this disagreement are, to date, not understood.

The very high value of our measured onset current (42 or 62 kA at 4 g/s of Argon, depending on whether anode depletion or strong unsteadiness is the criterion) is not inconsistent with the lower values obtained by other researchers, and appears to be dictated by geometrical differences. The anode depletion theory of Baksht et. al.[6] can be shown to predict

$$\frac{J^7}{\dot{m}^4} \sim \frac{L}{b^3 H^2} \tag{10}$$

where $b = \mu_o/4\pi \ln r_a/r_c$ is the thrust parameter, L, is the chamber length, and $H = r_a - r_c$ is the electrode spacing. For our thrusters, L = 9 cm, r_a = 7.25 cm, r_c = 6.35 cm, and $\dot{m}$ = 4 g/s, while for the Princeton Benchmark thruster, L = 6 cm, r_a = 5 cm, r_c = 1 cm, and $\dot{m}$ = 6 g/s. If we accept as an onset current for the Benchmark thruster the range J^* = 20–23 kA,[17] the corresponding scaled value for our case would be 47 to 55 kA, in fair correspondence with the data.

The electrothermal instability theory[15] also predicts increases of $(J^2/\dot{m})^*$ when the length increases, the interelectrode distance decreases, and the discharge perimeter increases—all of which occur in our case when comparing to the Benchmark thruster. The factors due to these effects can be estimated as 1.40, 1.50, and 2.1, respectively, which would yield $J^* = 38$–40 kA for our thrusters. This is indeed higher than for the Benchmark thruster but not as high as measured for reasons which are not currently understood.

We note that these annular channels clearly separate two types of effects which have in the past been together ascribed to a single onset phenomenson. From the efficiency standpoint, it is clear that operation with a depleted anode is unacceptable, but there seems to exist an operational regime between the onset of performance degradation, noted by anode related losses, and the onset of performance degradation by electrode erosion caused by catastrophic arcing.

Results of Interior Probing

Using the magnetic probes, maps of current streamlines were constructed for the higher currents before arcing onset (some data were also taken at lower currents, but they are less reliable due to the difficulty in guaranteeing a symmetric discharge). Using these data (Fig. 8), one can construct plots of current density along the cathode surface versus axial distance. These are shown in Fig. 9 for all three channels. It is clear that the strong current concentration at the exit of the constant area channel is greatly reduced in both flared channels (PFC, FFC), especially in the PFC. The FFC also shows a reduced inlet current concentration when compared to either the CAC or the PFC, which have a constant upstream separation. The current displaced from this peak is redistributed throughout the rest of the FFC, thus contributing to the higher level seen downstream when compared to the PFC. These results are in qualitative agreement with theoretical predictions. That the reduction in the inlet and exit current concentrations does reduce overall dissipation is indicated by electron temperature profiles as measured by Kilfoyle.[12,13]

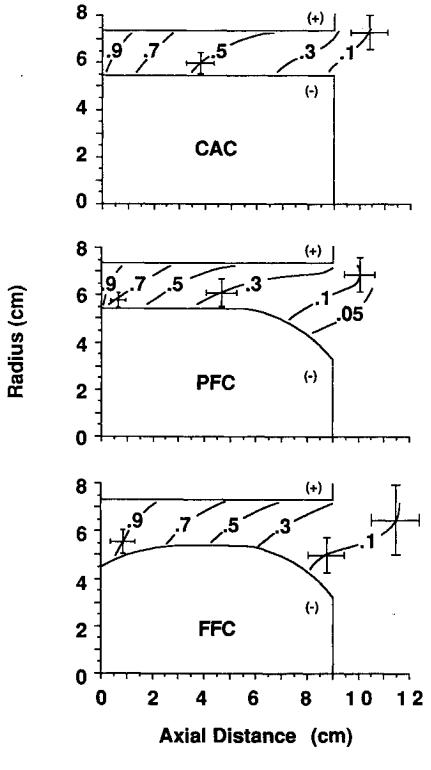

Fig. 8 Normalized current contours (fraction of the total thruster current) in the three MPD arcjet channels at 59 kA.

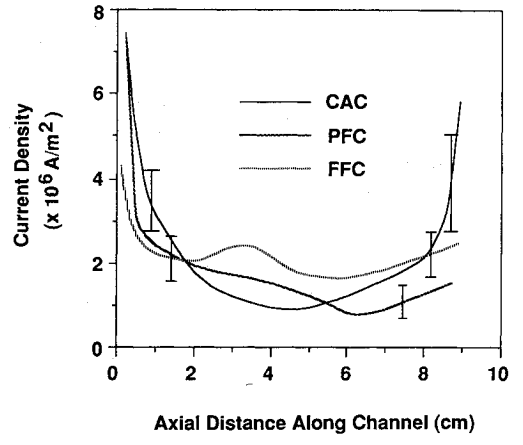

Fig. 9 Calculated current density variations along the three MPD arcjet cathodes.

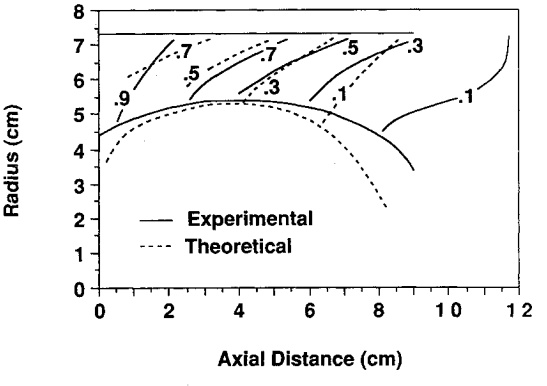

Fig. 10 Comparison of the experimental FFC normalized current contours (fraction of the total thruster current) with the theoretically determined contours for a 59 kA MPD arcjet channel.

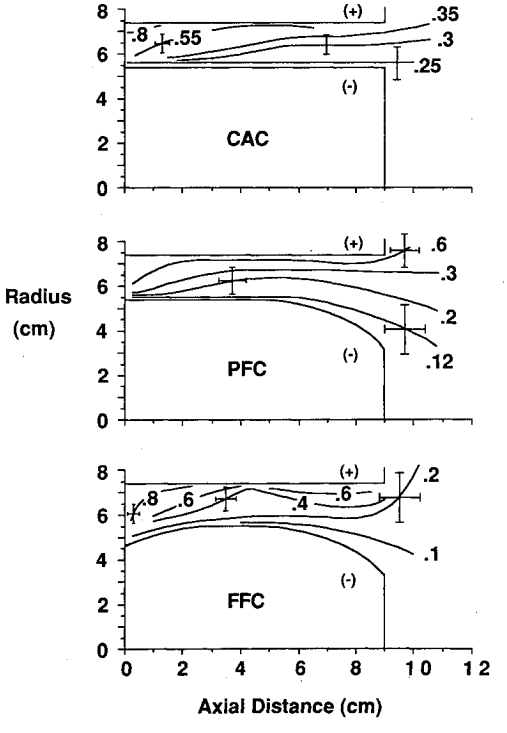

Fig. 11 Normalized floating potential contours (floating potential/terminal voltage) in the three experimental MPD arcjets.

A direct comparison between experimental and theoretical current distributions is made difficult by the fact that the data are for a current level higher than the design current. In Fig. 10, the experimental current lines in the FFC at 60 kA (solid lines) have been overlaid on those for a hypothetical channel designed for 60 kA (broken lines). Aside from the slight change in channel contour, and from the greater extent of the outside current "spillage" in the experimental data, there is a fair correspondence, particularly regarding the slopes of the lines (related to the local Hall parameter). Two obvious sources of theoretical errors are the presence in the experimental channel of a large and axially nonconstant anode drop and the neglect of the initial ionizing region in the theoretical arcjet. It can be seen from the equipotential map for each real channel, in Fig. 11, that the anode voltage drop is not constant and is maximum near the throat.

Conclusions

Several effects of area variation have been experimentally documented, and the predicted reduction of dissipation at inlet and exit due to a convergent-divergent geometry has been confirmed, at least qualitatively. Anode depletion was noted near the current level predicted by a modified form of Baksht's theory, but a stable region of postdepletion operation was also observed, terminating in large scale instability in the case of the divergent channels. On the basis of previous analyses, it is argued that the electrothermal instability associated with near full ionization may be the cause of this last phenomenon. If so, our tests would have confirmed *both* competing theories of onset (based on anode depletion and full ionization, respectively). Interesting design guidelines may follow from the reality of both effects, i.e., the designer would strive to force them to coincide so as to maximize the useful operating range. However, more detailed work needs to be done to verify or disprove these interpretations.

References

[1]Heimerdinger, D. J., Kilfoyle, D. B., Martinez-Sanchez, M. M., "Experimental Characterization of Contoured Magneto Plasmadynamic Thrusters," AIAA Paper 88-3205, Boston, MA, 1988.

[2]Cobine, J. D., *Gaseous Conductors*, Dover Publications, New York, 1958.

[3]Rudolph, L. K., and Jahn, R. G., "The MPD Thruster Onset Current Performance Limitation," Ph.D. Dissertation, Department of Mechanical and Aerospace Engineering, Princeton University, Princeton, NJ, 1980.

[4]Hugel, H. "Effect of Self-Magnetic Forces on the Anode Mechanism of a High Current Discharge," *IEEE Transactions on Plasma Sciences*, PS-8(4), 1980, pp. 437–442.

[5]Kuriki, K., Onishi, M., and Morimoto, S., "Thrust Measurement of KIII MPD Arcjet," *AIAA Journal*, Vol. 20, No. 10, 1982, p. 1414.

[6]Baksht, F. G., Moizhes, B. Ya, and Rybakov, A. B., "Critical Regime of Plasma Accelerator," *Soviet Physics*, Vol. 18, No. 12, 1974, p. 1613.

[7]Choueiri, E. Y., Kelly, A. J., and Jahn, R. G., "MPD Thruster Plasma Instability Studies," AIAA Paper 87-1067, Colorado Springs, CO, 1987.

[8]Schrade, H. O., Auweter-Kurtz, M., and Kurtz, H. L., "Cathode Phenomena In Plasma Thrusters," AIAA Paper 87-1096, Colorado Springs, CO, 1987.

[9]Turchi, P. J., "Critical Speed and Voltage-Current Characteristics in Self-Field Plasma Thrusters," *Journal of Propulsion and Power*, Vol. 2, No. 5, 1986, pp. 398–401.

[10]Heimerdinger, D. J., and Martinez-Sanchez, M., "Two Dimensional Analysis of an MPD Arcjet," AIAA Paper 85-2400, Alexandria, VA, 1985.

[11]Heimerdinger, D. J., "Fluid Mechanics in a Magnetoplasmadynamic Thruster," Ph.D. Dissertation, Massachusetts Institute of Technology, Department of Aeronautics and Astronautics, Cambridge, MA, 1988.

[12]Kilfoyle, D. B., "Spectroscopic Analysis of a Magnetoplasmadynamic Arcjet," Masters Thesis, Massachusetts Institute of Technology, Department of Aeronautics and Astronautics, Cambridge, MA, 1988.

[13]Kilfoyle, D. B., Martinez-Sanchez, M., Heimerdinger, D. J., and Shepard, E., "Spectroscopic Investigation of the Exit Plane of and MPD Thruster," IEPC-88-027, Garmisch-Partenkirchen, Germany, 1988.

[14]Heimerdinger, D. J., and Martinez-Sanchez, M., "Fluid Mechanics in a Magnetoplasmadynamic Thruster," IEPC-88-039, Garmisch-Partenkirchen, Germany, 1988.

[15]Niewood, E., Preble, J., Hastings, D. E., and Martinez-Sanchez, M., "Electrothermal and Modified Two-Stream Instabilities in MPD Thrusters," AIAA Paper 90-2607, Orlando, FL, 1990.

[16]Martinez-Sanchez, M., "The Structure of Self-Field Accelerated Plasma Flows," Journal of Propulsion and Power, Vol. 7, No. 1, 1991, pp. 56–64.

[17]Burton, R. L., Clarke, K. E., and Jahn, R. G., "Thrust and Efficiency of a Self Field MPD Thruster," AIAA Paper 81-0684, Las Vegas, NV, 1981.